Hindawi
Journal of Nanotechnology
Volume 2022, Article ID 2288892, 11 pages
https://doi.org/10.1155/2022/2288892

Research Article

Impact of Deacetylation Degree on Properties of Chitosan for Formation of Electrosprayed Nanoparticles

Hien Thi-Thanh Nguyen,[1,2,3] Tinh Ngoc Tran,[3] Anh Cam Ha,[1,2] and Phu Dai Huynh[1,4,5,6]

[1]*Vietnam National University Ho Chi Minh City, Linh Trung Ward, Thu Duc District, Ho Chi Minh City, Vietnam*
[2]*Faculty of Chemical Engineering, Ho Chi Minh City University of Technology, Vietnam National University Ho Chi Minh City, 268 Ly Thuong Kiet Street, District 10, Ho Chi Minh City, Vietnam*
[3]*Faculty of Chemical Engineering, Ho Chi Minh City University of Food Industry, 140 Le Trong Tan Street, Tan Phu District, Ho Chi Minh City, Vietnam*
[4]*Faculty of Materials Technology, Ho Chi Minh University of Technology, Vietnam National University Ho Chi Minh City, 268 Ly Thuong Kiet Street, District 10, Ho Chi Minh City, Vietnam*
[5]*National Key Laboratory of Polymer and Composite Materials, Ho Chi Minh University of Technology, Vietnam National University Ho Chi Minh City, 268 Ly Thuong Kiet Street, District 10, Ho Chi Minh City, Vietnam*
[6]*Research Center for Polymeric Materials, Ho Chi Minh University of Technology, Vietnam National University Ho Chi Minh City, 268 Ly Thuong Kiet Street, District 10, Ho Chi Minh City, Vietnam*

Correspondence should be addressed to Phu Dai Huynh; hdphu@hcmut.edu.vn

Received 11 October 2021; Revised 11 April 2022; Accepted 15 April 2022; Published 26 May 2022

Academic Editor: Sivakumar Manickam

Biopolymer of natural origin as chitosan has been studied and applied widely in practice. In the pharmaceutical field, especially, chitosan nanoparticles have been researched for a variety of drug delivery systems. There are many factors influencing the success of the chitosan nanoparticle delivery system. Therein, the specific parameters to the physicochemical nature of chitosan greatly determine the efficiency of its drugs carrier. The degree of deacetylation (DD) of chitosan is one of those parameters. In this study, the influence of DD on chitosan properties was clarified to facilitate the preparation of nanoparticles by the electrospraying method. DD can affect the solubility, crystallinity, and surface tension of chitosan, but it cannot strongly impact the viscosity of chitosan solution as much as the molecular weight (Mv). From these results, M3 chitosan, owning a high DD of 86.70%, and crystalline index of 44%, was dissolved in acetic acid for the collection of electrosprayed nanoparticles. The M3 solution having low viscosity of under 50 mm^2/s displayed the easy adjustment of the stable Taylor-cone droplet at the nozzle tip. Particularly, the M3 chitosan solution with a concentration of 1.5 wt.% in acetic acid of 90 wt.% concentration operated at the working condition of 12 kV voltage, a distance between the two electrodes of 10 cm created spherical particles with an average diameter of 338 nm, narrow size distribution. These chitosan nanoparticles can obtain the initial requirement for application as injectable drugs carrier.

1. Introduction

Polymeric nanoparticles have been used in academic research and employed extensively in some practical fields. Generally, nanoparticles are solid, colloidal particles containing macromolecular materials with a nanometer size from 10 nm to 1000 nm [1, 2]. They show more special properties than bulk particles. One of the crucial features at the nanosize level is the large surface area to volume ratio. This is useful in applications like adsorption or loading of therapeutic agents. As a result, nanoparticles are considered a potential drug delivery system in the pharmacy field [1, 3–7]. They have been used to encapsulate some medicinal agents, such as vitamins, probiotics, protein, bovine serum albumin, doxorubicin, insulin (chitosan nanoparticles), ciprofloxacin, curcumin (poly (lactide-co-glycolide)

nanocapsules), palmarosa oil, and geraniol (poly(Ɛ-caprolactone) nanoparticles) [2–7].

There are many methods to create nanoparticles like ionic gelation, emulsion, solvent evaporation, reverse micelles, self-assembling, and spray drying [3–7]. Among those, electrospraying is an attractive technique applied in the formation of drug carriers. It reduces the denaturation of protein drugs by using less solvent. Besides, it is low-cost, simple, and a one-step process. Moreover, electrospraying and electrospinning, which belong to electrohydrodynamic techniques, are now moving forward with diverse procedures such as single-fluid blending, side-by-side, and coaxial. Therefore, the electrospraying method for preparing and developing material nanostructures will go further [8–24]. The main principle of this method is based on the theory of charged droplets. The polymer solution is moved to a metallic nozzle by a syringe pump. With the high voltage applied between the metallic nozzle and a collector, the liquid droplet at the nozzle tip has high electric charges and a result of that is the generating of electrostatic force. When this force overcomes the surface tension of the liquid drop, a jet is formed and breaks up the primary droplet into smaller droplets. They fly towards a counter electrode (the collector) and form dispersed nanoparticles by Coulomb electrostatic repulsion and solvent evaporation during the flight to the collector. According to [8–14], two main kinds of variables affect the formation of nanoparticles in the electrospraying method, consisting of material properties and operational parameters. Some factors present in the working apparatus, like the voltage, tip-collector distance, needle diameter, and flow rate. Meanwhile, the quantities such as polymer concentration, polymer molecular weight, solvent concentration, viscosity, conductivity, and surface tension are material features. In fact, the electrospraying method is sensitive to small changes in these mentioned factors to form different modes at the nozzle tip, such as dripping, spindle, multijet, and the Taylor-cone. However, creating a solid, uniform nanoparticle is only shown in the stable Taylor-cone mode. Therefore, all these material features and working conditions need to be considered carefully to obtain the desired particles, especially the properties of the chosen material.

Biomaterials obtained from natural polymers have been consumed widely in pharmaceutical technology. They have advantages: less toxic, biocompatible, and biodegradable. Chitosan is a natural polymer whose composition has a carbohydrate backbone structure consisting of two types of repeating units, N-acetyl-d-glucosamine and d-glucosamine, linked by (1–4)-β-glycosidic linkage. Chitosan is produced from the deacetylation of chitin, an abundant polysaccharide from crustacean shells [3, 5, 6]. The degree of deacetylation (DD) is described as a molar percent of the D-glucosamine compared with the total D-glucosamine and N-acetyl-D-glucosamine in the chain. It is an important factor of chitosan because it influences the physicochemical features of chitosan. DD can affect the solubility, crystallinity, even viscosity, and the surface tension of chitosan [6, 25–28]. It is necessary to analyze the impact of DD on chitosan's relevant properties to apply the material to a specific field.

There have been published topics on chitosan nanoparticles by the electrospraying method. They focused mainly on the chitosan molecular weight (Mw) and concentration as characteristic chitosan [8–12, 14]. Mw was considered one of the factors that can significantly influence the viscosity of chitosan solution and be relative to chitosan concentration (the critical overlap concentration). High Mw chitosan often generates a high viscosity solution. It is also noted that a stable Taylor-cone mode is observed for solutions having concentrations between a critical overlap concentration and an entanglement concentration and low viscosity (<64 cP) [9, 11, 29]. Although DD can affect the properties of chitosan, research on the effect of DD on the electrospraying process to collect nanoparticles has not been mentioned. Besides, the polymeric materials applied in advanced electrohydrodynamic techniques are limited. It is necessary to modify previous materials or find new materials. Herein, chitosans with various DD were investigated about the processability using the electrospraying method. This information can be useful data in future studies about coaxial and side-by-side electrospraying to create new nanostructures.

In this study, the role of DD on the capacity of solubility, crystallinity, viscosity, and surface tension of chitosans was investigated. On an expectation, the chitosan solution for the electrospraying process must be homogeneous and not have too high viscosity and surface tension for easy nanoparticle collection. Several analytical methods containing acid-base titration, FTIR, XRD, turbidity, and viscosity were used to determine the characteristic of chitosan. Additionally, the experiments forming chitosan nanoparticles by electrospraying apparatus were tested. With the aim of the chitosan nanoparticles applied in an injectable drug delivery system, the expected size is under 500 nm. The morphology of the nanoparticles was evaluated by SEM. The contact angles of chitosan solution and the size distribution of particles were examined by Image J and Minitab software. Hoping to evaluate the impact of DD on chitosan solution can effectively control the spraying process to make desired chitosan nanoparticles.

2. Materials and Methods

2.1. Materials. There are three types of chitosan from different origins: Sigma-Aldrich, Acros Organics, and Vietnam. Acetic acid, hydrochloric acid, and sodium hydroxide are purchased from Xilong (China).

2.2. Methods

2.2.1. Apparatus Design and Experimental Setup. The electrospraying apparatus operates with a voltage up to 25 kV, a syringe pump at a flow rate of 0.1 mL h^{-1}, an 18G needle (inner diameter 0.838 mm), and a collector (an alumina foil). First, chitosan was stirred in an acetic acid 90 wt.% concentration to obtain a homogeneous mixture. The chitosan solution had experimented with a set of changed concentrations from 1 wt.% to 2 wt.%. The solution was sprayed within the investigation range of the potential and the

distance from the nozzle to the collector. In the process, the droplets of chitosan solution at the tip were taken images by a microscope. The nanoparticles were deposited on the alumina foil, dried under a vacuum before taking the scanning electron microscopy (SEM).

2.3. Characterization of the Chitosan. The degree of deacetylation (DD) of chitosan was determined by the acid-base titration method with methyl orange as an indicator. According to [28, 30, 31], 0.5 g of dry chitosan was exactly weighted and dissolved in 0.1 M HCl. After that, the solution was added two to three drops of 1.0 wt.% of the indicator and titrated by 0.1 M NaOH. At the equivalence point, the color solution had transitioned from red to orange-yellow.

DD was calculated as follows:

$$\%NH_2 = \frac{\left(C_{\mathrm{HCl}} \times V_{\mathrm{HCl}} - C_{\mathrm{NaOH}} \times V_{\mathrm{NaOH}}\right) \times 0.016 \times 100}{m_{chitosan}}, \quad (1)$$

$$\%DD = \frac{\%NH_2 \times 100}{9.94}. \quad (2)$$

Structures of chitosans were analyzed by Fourier-transform infrared spectroscopy (FTIR) on a Frontier of Perkin Elmer spectrophotometer. The polymers were mixed with KBr and pressed to a plate for measurement.

Turbidimetric measurement for chitosan solubility at different pH values was determined by a Milwaukee Mi415 Turbidity Meter. Briefly, the chitosan solutions were formed by dissolving 0.1 g chitosan in 20 mL HCl 0.1 M and adjusted slowly the pH value by NaOH 0.1 M [32]. All experiments were performed in triplicate, and each value is the average of three measurements.

The crystalline phase of chitosans was measured by X-ray diffraction (XRD). The spectrometries were obtained by using the powder diffraction meter with Cu-Ka radiation in the range 5–70° (2θ). The crystalline index (CrI, %) was determined as follows:

$$(\%)CrI = \frac{I_{110} - I_{\mathrm{am}}}{I_{110}} \times 100, \quad (3)$$

where I_{110} is the maximum intensity of the diffraction pattern at 20°, and I_{am} is the intensity of amorphous diffraction at 16°[33].

The contact angles of chitosan solutions were determined by handling the images of chitosan droplets on the smooth glass pieces with ImageJ software.

The viscosity-average molecular weight of chitosan (Mv) was determined by the Mark-Houwink equation:

$$[\eta] = 1.81 \cdot 10^{-3} \cdot M_{\mathrm{v}}^{0.93}, \quad (4)$$

where [η] is the intrinsic viscosity measured by a capillary viscometer following the procedure of the previous documents [9, 29, 34]. 0.1 M acetic acid/0.2 M NaCl was used as a solvent to dissolve chitosans.

The kinematic viscosity of chitosan solution was determined by the capillary viscometer at 25°C. The flow time of the solution was measured five times. The time value calculated the average of five measurements and converted them to kinematic viscosity by using a calibrated viscometer constant.

2.4. Characterization of the Chitosan Nanoparticles. The morphologies of chitosan particle surfaces were studied by scanning electron microscopy (SEM-S4800 HITACHI). Size distributions of the nanoparticles were analyzed by ImageJ and MiniTab software.

3. Results and Discussion

3.1. Effect of the DD on the Characterization of Chitosan. Three kinds of chitosan are denoted as M1, M2, and M3, corresponding to their brands of Sigma-Aldrich, Vietnam, and Acros Organics. The results of DD were displayed in Table 1. All samples have DD values over 70%, in that M3 has the highest DD with 86.70%. It implies that there are more $-NH_2$ groups in their structures.

According to [3–6], chitosan can dissolve well in a pH under 6.0 by the protonation of NH_2 to form NH_3^+. That means the more NH_2 groups in the chain of chitosan structure are, the easier solubility of chitosan solution in the pH acid environment is. In this study, to evaluate the solubility of chitosan, all samples were dissolved in 0.1 M HCl solution, then adjusted pH from 2.0 to 8.0 at the same conditions for turbidity measuring. In observation, all three solutions were transparent at pH = 2.0, but the turbidity value of the M3 solution was nearly zero, while those of M1 and M2 were 30 FNU. In Figure 1, the profiles are the same shapes with the FNU value stability in the pH range from 2.0 to 6.0 and increase sharply to about 430 FNU at pH = 7.0. It proves that M3 has better purity and solubility than M1 and M2. The good solubility of M3 is related to high DD due to more $-NH_2$ hydrophilic groups in its structure.

The crystallinity of chitosan was evaluated through X-ray diffraction patterns and CrI (crystalline index). As shown in Figure 2, the results of the XRD analysis display all of the samples presenting a strong characteristic peak at 2θ around 20° (amine II "$-NH_2$") [33]. Besides, M1 and M2 also have a high intensive peak at 10°(amine I "$-N-CO-CH_3$"), whereas this peak disappears completely in M3. Particularly, M2 is an additional shoulder in 21°. It can estimate that the crystalline degree of M2 and M1 is larger than M3. Comparative with the intensities of diffraction peaks, the peaks of M2 are higher and sharper than those of M1 and M3. From those, it can be concluded that M2 has a better degree of crystallinity than M1 and M3 and is consistent with calculated CrI values from samples M1, M2, and M3 to be 60%, 78%, and 44% respectively. It considers a relation between the DD value and the crystallinity of M3. With high DD values, M3 does not have more acetyl groups in its structure, which causes decreasing intermolecular hydrogen linkages that occurred by the hydroxyls and acetyl groups between two intersheets of its parallel arrangement as a reason for disappearing the peak at 10° [33]. As a result, it leads to a low crystalline degree of M3. Meanwhile, M1 and M2 have both inter/

Table 1: DD values of the chitosans.

Chitosan	M1	M2	M3
DD (%)	76.13 ± 1.88	80.61 ± 2.35	86.70 ± 2.63

Effect of the DD on the solubility of chitosan.

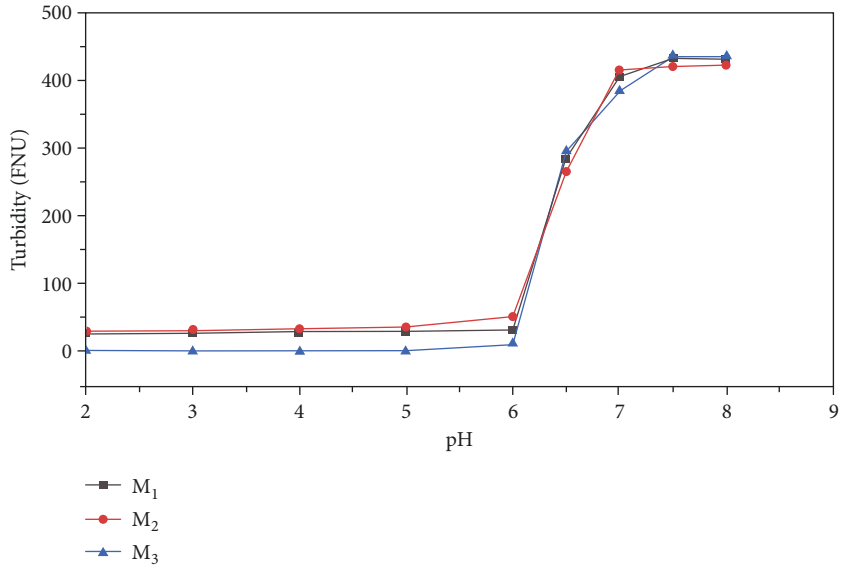

Figure 1: The turbidity of chitosan solution at different pH. Effect of the DD on the crystallinity and structure of chitosan.

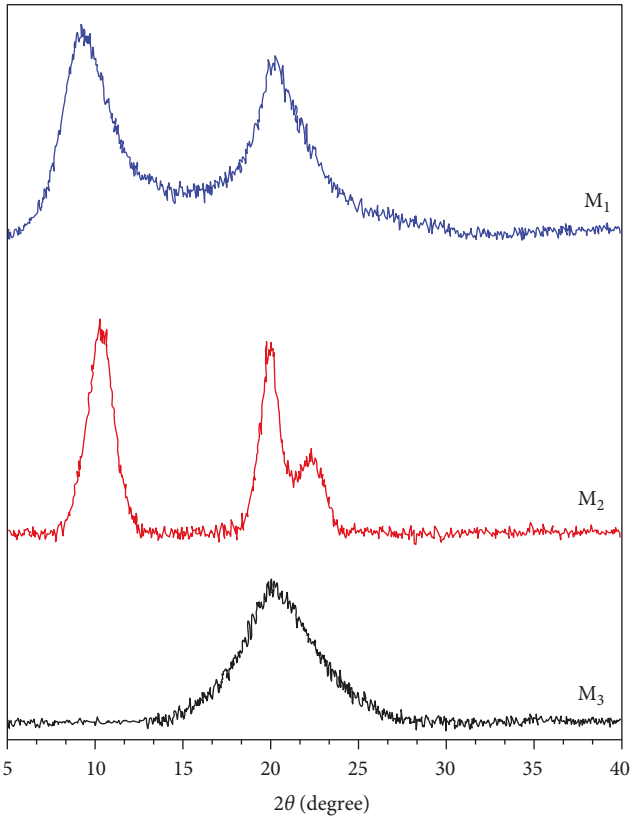

Figure 2: XRD of M1, M2, and M3.

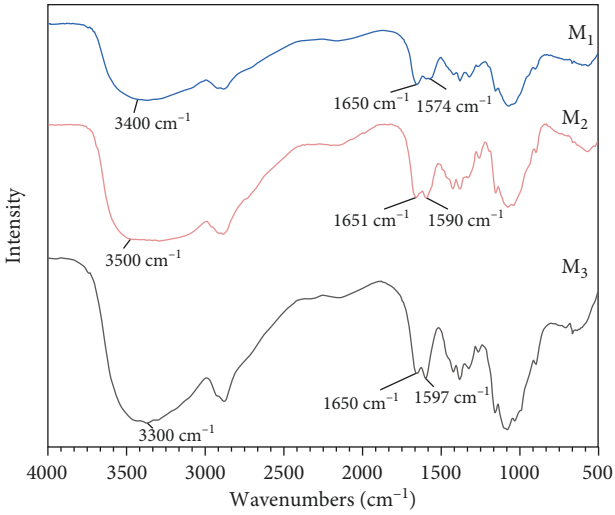

Figure 3: FTIR spectra of M1, M2, and M3. Effect of the DD on the surface tension of chitosan solution.

intramolecular hydrogen bonds of H_2N--OH and CHO--OH as a trend of these reports [25, 26].

FTIR spectra display the characteristic functional groups of chitosan structures in Figure 3. In general, all chitosan FTIR profiles have the same shape with typical absorption peaks, including the band 3300–3500 cm^{-1} (–OH group), 1650 cm^{-1} (–C=O in acetamide group), and 1590 cm^{-1} ($–NH_2$ group). In detail, the peaks of –OH groups are broad,

not sharp because of overlapping absorption peaks of the –OH and –NH groups or –OH and –CHO. Besides, the band at 1350 cm^{-1}, which is assigned to the vibrations of the amide $–CH_3$ group, disappears in all the spectra [35]. It shows the inter-intramolecular hydrogen bonding in the structures. Importantly, M1, M2, and M3 have different center wavenumber near 3400 cm^{-1}, 3500 cm^{-1}, and 3300 cm^{-1}, respectively. The higher the shift frequency is, the higher the structural arrangement order obtains [36]. Consequently, the higher-order structure of chitosans is arranged to M2, M1, and M3, correspondingly. Additionally, the M3 spectrum displays the band at 1590 cm^{-1} (amide 2) with a sharp peak than the 1650 cm^{-1} band (attributed to amide 1), while the M1 spectrum is already the opposite. It also demonstrates that there are many $–NH_2$ groups in the M3 structure, in contrast to the M1 structure. Furthermore, the band assigned amide 2 of M1 (1574 cm^{-1}) is located at a lower wavenumber than these of M2 and M3 (1590 cm^{-1}). It implies that there is a strong intramolecular hydrogen bonding in the structure, which leads to high crystallinity as mentioned in the XRD analysis [37]. The FTIR spectrum of M2 shows the presence of broad peaks of amides 1 and 2, which demonstrated the interaction of the functional groups. Perhaps, its geometric structure causes the formed inter-intramolecular hydrogen linkage more conveniently than the other chitosan, which induces good crystallinity.

In the electrospraying method, a droplet in the nozzle flies to the collector when the electric field force overcomes the surface tension of the solution. The higher the surface tension is, the more difficult the spraying process is. Note that increasing the surface tension leads to a larger contact angle [38]. Figure 4 shows the contact angle values of 1.0 wt.% chitosan solution in 90 wt.% of acetic acid decrease from M1 and M2 to M3 respectively, similar to the order decreasing surface tension. The contact angles of the chitosan solutions increase in the rule of the increasing chitosan concentrations in Figure 5. With the high DD, the M3 structure has a repulsion of positive charges, which leads to considerable expansion of polymer chains. So, the cohesive force of the M3 molecules is weak. Generally, all the chitosan solutions do not have too high contact angles because the chosen acetic acid solvent in the high concentration of 90 wt.% has a low surface tension.

The viscosity of polymer solution is an important parameter that greatly affects the ability to produce the nanoparticles by an electrospraying method. Adjusting the Taylor-cone nozzle to form round, uniform chitosan nanoparticles require a chitosan solution with appropriate viscosity. The too high or too low viscosity of chitosan causes drawbacks to control the spraying process. With low viscosity and high conductivity, the nanoparticles are often sprayed in multijet mode leading to poor size distribution. In contrast, the chitosan solution with high viscosity has some disadvantages: blocking of the nozzle, spraying type as a dripping mode, or using a high voltage to overcome the surface tension. As a result, the electrospray process is unstable as a reason for deforming shapes of particles [8,11].

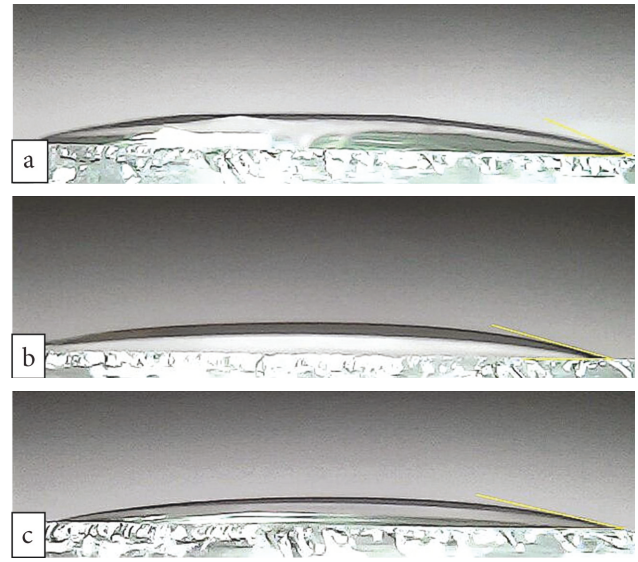

Figure 4: Images of contact angles of 1.0 wt.% chitosan solution: (a) M1, (b) M2, and (c) M3.

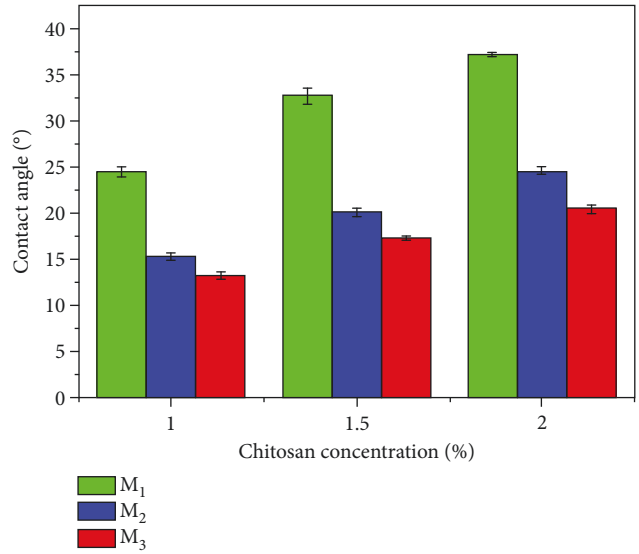

Figure 5: The contact angle of chitosan solution in different concentration. Effect of the DD on the viscosity of chitosan solution.

The viscosities of 1.0 wt.% chitosan concentration in acetic acid 90 wt.% are illustrated in Figure 6. M1 reached the highest viscosity of 210.52 mm^2/s, ten times that of M2, while M3 obtained the lowest value of 13.96 mm^2/s.

According to [39], the high DD chitosan has high viscosity because of the inter-intramolecular hydrogen bonds formed by amino and hydroxyl groups. However, this study is not compatible with this trend. Although M3 has the highest DD, its structure is less hydrogen linkage, as demonstrated in the FTIR and XRD analysis. Therefore, it can be explained that M3 viscosity is the lowest. On the other hand, the DD value of M1 (76.13%) is close to M2 (80.61%), and the CrI is smaller, but M1 chitosan was difficult to dissolve and had high viscosity. In observation, increasing

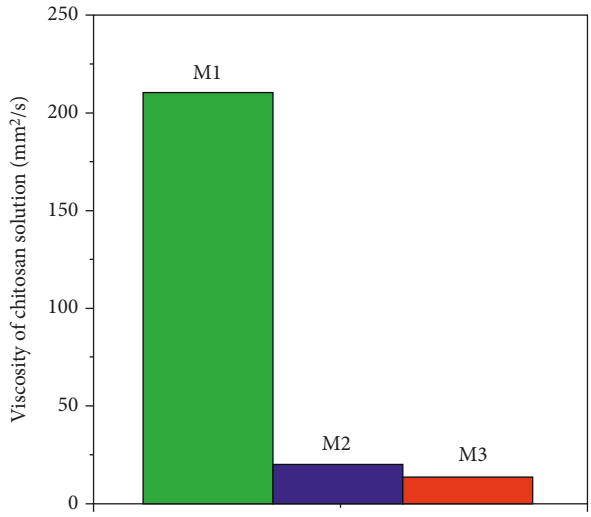

Figure 6: The viscosity value of 1.0 wt.% chitosan concentration in 90 wt.% acetic acid concentration.

Table 2: The viscosity-average molecular weight (Mv) values of the chitosan.

Chitosan	M1	M2	M3
Mv (kDa)	741	516	421

the concentration of chitosan to 1.5 wt.% and 2.0 wt.%, the viscosity of M1 increased very high, and M1 did not dissolve completely. It seems to be related to the strong intramolecular hydrogen as the FTIR analysis mentioned and the molecular weight of chitosan [9, 11]. Table 2 shows the highest Mv of 741 kDa of M1 and the lowest Mv of 421 kDa of M3. The results were suitable with the obtained values of the viscosity.

From the previously mentioned results, DD mainly influences the solubility of chitosan solution and lightly impacts crystallization and surface tension. High DD of 86% of M3 enhances the solubility, but the formation of NH_3^+ protons causes the molecular chain to expand as a result of reducing crystallinity and surface tension. Meanwhile, DD does not powerfully affect the viscosity of the solution, which is controlled by the molecular weight. The higher the molecular weight is, the higher the viscosity of the chitosan solution is. The concentration range for reproducible electrospraying of high molecular weight chitosan is limited [8, 11]. Obviously, both the deacetylation degree (DD) and molecular weight (Mw), two important parameters of chitosan, significantly influence the solution for nanoparticle generation by the electrospraying method.

Following the initial requirements of the chitosan solution, including a uniform solution, appropriate surface tension, and viscosity to use the electrospraying method, chitosan samples are ordered in decreasing levels: M3, M2, and M1. In Figure 7, with the 1.0 wt.% chitosan in 90 wt.% acetic acid concentration, the M3 solution seems better than the others.

3.2. Chitosan Nanoparticles Formed by the Electrospraying Method

3.2.1. Evaluating M1, M2, and M3 Particles. The experimental spraying was examined initially with 1.0 wt.% chitosan in 90 wt.% acetic acid concentration of M1, M2, and M3. As shown in Figures 8(a), 8(b), and 8(c), SEM images of M1, M2, and M3, selected based on the droplets as a Taylor-cone, displayed different morphology. The shapes of M1 particles were stacked, in contrast to round, separate particles of M2 and M3. Additionally, M1 and M2 solutions had to apply the high voltage (U) of 18 KV due to high viscosity. Particularly, the M1 solution was difficult to control the Taylor-cone. This point is similar to the prediction about the M1 sample because of its owing high Mv and viscosity.

Increasing to 2.0 wt.% chitosan concentration, M2 exhibited poor solubility and increased the viscosity to 126 mm^2/s shown in Figure 9, as opposed to M3 (56 mm^2/s). It spent much of the time dissolving M2 than M3. The results of SEM of M2 and M3 particles are illustrated in Figure 10. All the particles obtained round, dense particles, but the M3 particles were more homogeneous than M2. With lower DD and higher crystallinity, M2 had trouble from 2.0 wt.% chitosan concentration. Compared with M2, M3 displayed more advantages. Therefore, M3 was selected to investigate for experiments on the electrospraying device.

The M3 solution that consists of 1.5 wt.% concentration in 90 wt.% acetic acid concentration was investigated following a change of voltage (U) and distance from the needle to the collector (L). As shown in Figure 11, the shapes of droplets at the nozzle tip were photographed by a microscope. At the same short distance of 7 cm and 10 cm, increasing potential power from 9 kV to 18 kV, the droplet of chitosan solution changed from cone-jet to multijet, whereas, in the long-distance of 12 cm and 15 cm, the droplets formed in order of dripping, cone-jet, and multijet when increasing voltage. Observation of the droplet at the nozzle in increasing the distance from 7 cm to 15 cm at the same low voltage ($U = 9$ kV, 12 kV), the shapes of droplets were cone, spindle, and dripping, respectively. In the situation of high voltage ($U = 15$ kV, 18 kV), the droplets were in the order multijet, spindle. The rule is similar to reported documents [8, 11, 12]. That means the applied appropriate voltage must overcome the electrostatic force of the solution to pull the droplet out of the nozzle with a stable cone-jet. When the voltage is enough to get over the electrostatic force in the case of the long-distance and low voltage, the droplet appears in a dripping, spindle mode, as opposed to the situation in which high voltage and short distance result in a multijet mode.

Based on the images of droplets as Taylor cone in Figure 11, three working conditions selected to analyze SEM were $L = 7$ cm, $U = 9$ kV; $L = 10$ cm, $U = 12$ kV; $L = 12$ cm, $U = 15$ kV. In fact, with the low viscosity of 36.29 mm^2/s (Figure 9), controlling the Taylor-cone shape of the droplet was easy. All morphology of particles revealed spherical, dense shapes with a diameter under 500 nm in Figure 12.

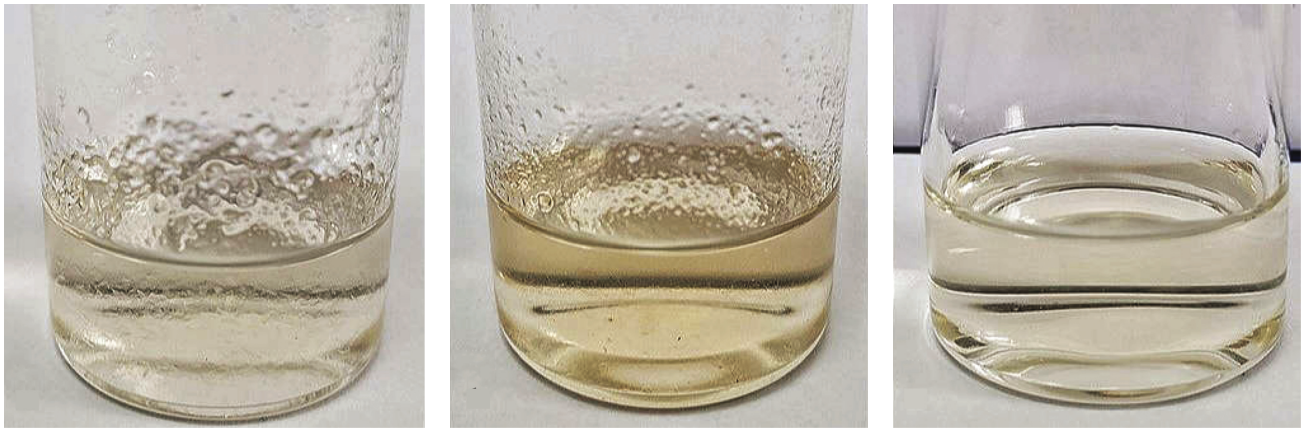

(a) (b) (c)

Figure 7: The solution of 1.0 wt.% chitosan in 90 wt.% acetic acid concentration: (a) M1, (b) M2, and (c) M3.

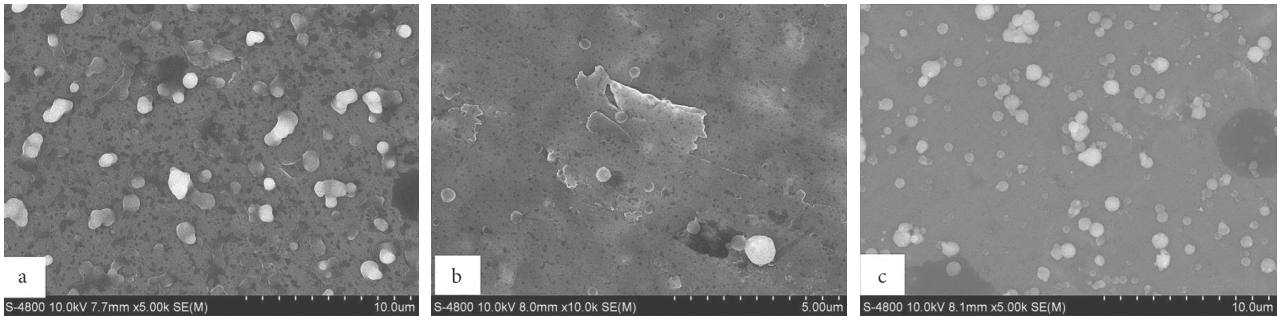

Figure 8: SEM images of the nanoparticles in 1.0 wt.% chitosan concentration at a different voltage (U) and distance (L). (a) M1 chitosan at $U = 18$ kV, $L = 12$ cm; (b) chitosan at $U = 18$ kV, $L = 12$ cm; (c) M3 chitosan at $U = 9$ kV, $L = 10$ cm.

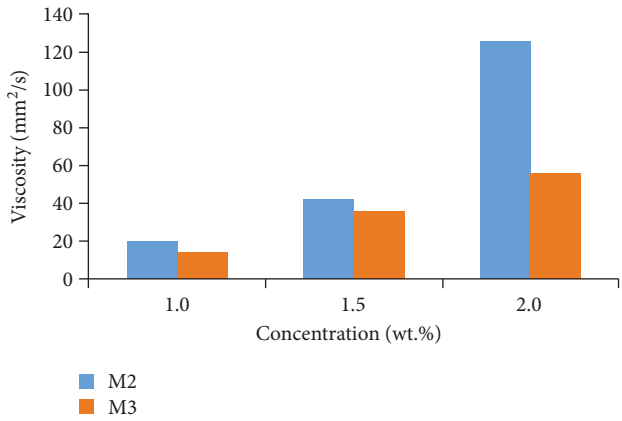

Figure 9: The viscosity of M2 and M3 chitosan solution in different concentrations.

Compared with the morphology particles of M3 chitosan solution from 1.0 wt.% to 2.0 wt.% concentration, the nanoparticles of M3 chitosan 1.5 wt.% concentration displayed more uniform at $U = 12$ kV and $L = 10$ cm with the average diameter of 338 nm in Figure 13. This size completely meets the requirement of nanoparticles for drug delivery systems.

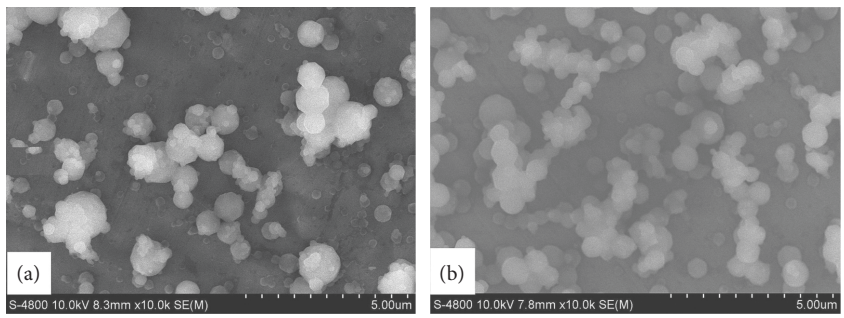

Figure 10: SEM images of the nanoparticles in 2.0 wt.% chitosan concentration at a different voltage (U) and distance (L). (a) M2 chitosan at $L = 12$ cm, $U = 18$ kV; (b) M3 chitosan at $L = 10$ cm, $U = 12$ kV. Effects of working parameters on M3 solution at 1.5 wt.% chitosan in 90 wt.% acetic acid.

Figure 11: Images of the droplets of 1.5 wt.% M3 chitosan concentration in 90 wt.% acetic acid concentration changing in different voltage (U) and distance (L).

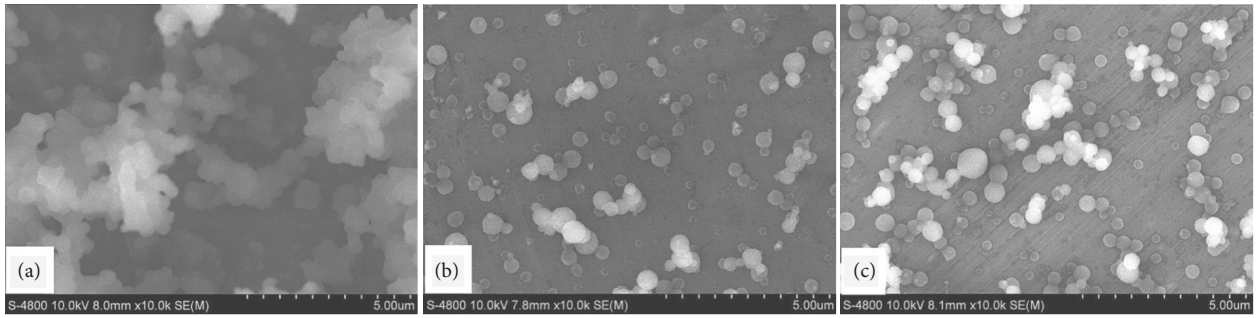

Figure 12: SEM images of 1.5 wt.% M3 chitosan concentration in 90 wt.% acetic acid concentration at a different voltage (U) and distance L. (a) $U = 9$ kV and $L = 7$ cm; (b) $U = 12$ kV and $L = 10$ cm; (c) $U = 15$ kV and $L = 12$ cm.

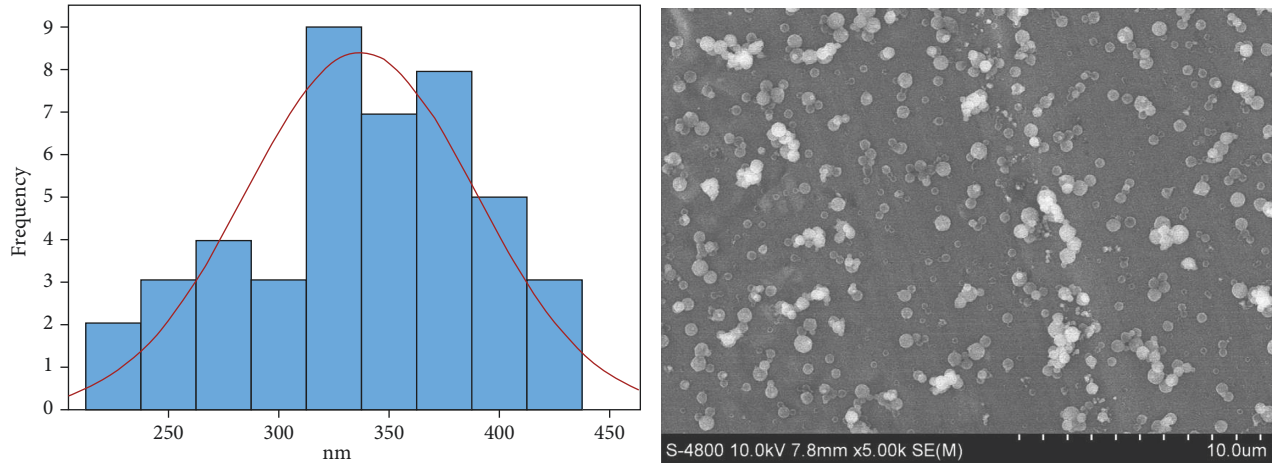

Figure 13: The size distribution and SEM image of 1.5 wt.% M3 chitosan concentration in acetic acid concentration of 90 wt.% at $U = 12$ kV, $L = 10$ cm.

4. Conclusion

In this work, the M3 chitosan with high DD (86.70%) contributed to good solubility, low crystallinity, and low surface tension. Additionally, the M3 solution has a low viscosity dominated by a small molecular weight. These two main factors made M3 chitosan favorable to apply in the electrospraying method. The results of SEM demonstrated that the obtained particles of M3 were spherical, dense with a diameter in nano size. Investigating process of the regime stable spraying was based on the initial observation of droplets at the nozzle as Taylor-cone. At the operational parameter of $L = 10$ cm, $U = 12$ kV, the particles of 1.5 wt.% M3 chitosan concentration in the acetic acid of 90 wt.% concentration had good morphology with an average diameter of about 338 nm. Thus, besides the Mv of chitosan, it is necessary to evaluate the DD value to produce chitosan nanoparticles by the electrospraying method.

Data Availability

The data used to support the finding of this study are included in the manuscript.

Conflicts of Interest

The authors declare that they have no conflicts of interest or personal relationships that could have appeared to influence the work reported in this paper.

Acknowledgments

The authors acknowledge the support of time and facilities from Ho Chi Minh City University of Food Industry and Ho Chi Minh City University of Technology (HCMUT), VNU-HCM. This research was funded by the Ministry of Science and Technology under the grant Scientific and Technological Mission according to the Vietnam-Korea Protocol (NĐT.27.KR/17) and supported by the Basic Science Research Program through grants from the National Research Foundation (NRF) of Korea, funded by the Korean Government (MEST) (2010-0027955 and NRF-2017R1D1A1B03028061).

References

[1] R. Singh, J. W. Lillard Jr., and J. W. Lillard, "Nanoparticle-based targeted drug delivery," *Experimental and Molecular Pathology*, vol. 86, no. 3, pp. 215–223, 2009.

[2] S. Bhattacharjee, "Polymeric nanoparticles," *Principles of Nanomedicine*, Jenny Stanford Publishing, New York, NY, USA, pp. 195–240, 2019.

[3] L. P. Gomes, V. M. F. Paschoalin, and E. M. Del Aguila, "Chitosan nanoparticles: production, physicochemical characteristics and nutraceutical applications," *Revista Virtual de Quimica*, vol. 9, no. 1, pp. 387–409, 2017.

[4] T. A. Ahmed and B. M. Aljaeid, "Preparation, characterization, and potential application of chitosan, chitosan derivatives, and chitosan metal nanoparticles in pharmaceutical drug delivery," *Drug Design, Development and Therapy*, vol. 10, pp. 483–507, 2016.

[5] V. Mikušová and P. Mikuš, "Advances in chitosan-based nanoparticles for drug delivery," *International Journal of Molecular Sciences*, vol. 22, no. 17, pp. 9652–9693, 2021.

[6] C. Saikia and P. Gogoi, "Chitosan: a promising biopolymer in drug delivery applications," *Journal of Molecular and Genetic Medicine*, vol. s4, 2015.

[7] C. Adhikari, "Polymer nanoparticles-preparations, applications and future insights: a concise review," *Polymer-Plastics Technology and Materials*, vol. 60, no. 18, pp. 1996–2024, 2021.

[8] M. Abyadeh, A. A. Karimi Zarchi, M. A. Faramarzi, and A. Amani, "Evaluation of factors affecting size and size distribution of chitosan-electrosprayed nanoparticles," *Avicenna Journal of Medical Biotechnology*, vol. 9, no. 3, pp. 126–132, 2017.

[9] D. V. H. Thien, S. W. Hsiao, and M. H. Ho, "Synthesis of electrosprayed chitosan nanoparticles for drug sustained release," *Nano Life*, vol. 02, no. 01, Article ID 1250003, 2012.

[10] J. A. Tapia-Hernández, P. I. Torres-Chavez, B. Ramirez-Wong et al., "Micro- and nanoparticles by electrospray: advances and applications in foods," *Journal of Agricultural and Food Chemistry*, vol. 63, no. 19, pp. 4699–4707, 2015.

[11] N. Bock, T. R. Dargaville, and M. A. Woodruff, "Electrospraying of polymers with therapeutic molecules: state of the art," *Progress in Polymer Science*, vol. 37, no. 11, pp. 1510–1551, 2012.

[12] A. Smeets, C. Clasen, and G. Van den Mooter, "Electrospraying of polymer solutions: study of formulation and process parameters," *European Journal of Pharmaceutics and Biopharmaceutics*, vol. 119, pp. 114–124, 2017.

[13] M. Kurakula and N. Raghavendra Naveen, "Electrospraying: a facile technology unfolding the chitosan based drug delivery and biomedical applications," *European Polymer Journal*, vol. 147, Article ID 110326, 2021.

[14] A. Í. S. Morais, E. G. Vieira, S. Afewerki et al., "Fabrication of polymeric microparticles by electrospray: the impact of experimental parameters," *Journal of Functional Biomaterials*, vol. 11, no. 1, p. 4, 2020.

[15] T. He and J. V. Jokerst, "Structured micro/nano materials synthesized: via electrospray: a review," *Biomaterials Science*, vol. 8, no. 20, pp. 5555–5573, 2020.

[16] R. Jatal, R. Osman, W. Mamdouh, and G. A. S. Awad, "Lung targeted electrosprayed chitosan nanocomposite microparticles boost the cytotoxic activity of magnolol," *Carbohydrate Polymer Technologies and Applications*, vol. 2, p. 100169, 2021.

[17] M. Roso, A. Lorenzetti, C. Boaretti, and M. Modesti, "Electrically conductive membranes obtained by simultaneous electrospinning and electrospraying processes," *Journal of Nanomaterials*, vol. 2016, Article ID 8362535, 11 pages, 2016.

[18] J. Hou, Y. Yang, D. G. Yu et al., "Multifunctional fabrics finished using electrosprayed hybrid Janus particles containing nanocatalysts," *Chemical Engineering Journal*, vol. 411, Article ID 128474, 2021.

[19] X. Cui, X. Li, Z. Xu et al., "Fabrication and characterization of chitosan/poly(Lactic-Co-glycolic acid) core-shell nanoparticles by coaxial electrospray technology for dual delivery of natamycin and clotrimazole," *Frontiers in Bioengineering and Biotechnology*, vol. 9, pp. 1–13, 2021.

[20] D. Li, M. Wang, W. L. Song, D. G. Yu, and S. W. A. Bligh, "Electrospun janus beads-on-a-string structures for different types of controlled release profiles of double drugs," *Biomolecules*, vol. 11, no. 5, Article ID 635, 11 pages, 2021.

[21] H. Lv, D.-G. Yu, M. Wang, and T. Ning, "Nanofabrication of janus fibers through side-by-side electrospinning - a mini review," *Materials Highlights*, vol. 2, no. 1–2, p. 18, 2021.

[22] K. Zhao, Z. H. Lu, P. Zhao, S. X. Kang, Y. Y. Yang, and D. G. Yu, "Modified tri–axial electrospun functional core–shell nanofibrous membranes for natural photodegradation of antibiotics," *Chemical Engineering Journal*, vol. 425, Article ID 131455, 2021.

[23] Y. Liu, S. Li, H. Li et al., "Synthesis and properties of core-shell thymol-loaded zein/shellac nanoparticles by coaxial electrospray as edible coatings," *Materials & Design*, vol. 212, p. 110214, 2021.

[24] T. Ning, Y. Zhou, H. Xu, S. Guo, K. Wang, and D. G. Yu, "Orodispersible membranes from a modified coaxial electrospinning for fast dissolution of diclofenac sodium," *Membranes*, vol. 11, no. 11, p. 802, 2021.

[25] C. Wenling, J. Duohui, L. Jiamou, G. Yandao, Z. Nanming, and Z. Xiufang, "Effects of the degree of deacetylation on the physicochemical properties and Schwann cell affinity of chitosan films," *Journal of Biomaterials Applications*, vol. 20, no. 2, pp. 157–177, 2005.

[26] J. Nunthanid, S. Puttipipatkhachorn, K. Yamamoto, and G. E. Peck, "Physical properties and molecular behavior of chitosan films," *Drug Development and Industrial Pharmacy*, vol. 27, no. 2, pp. 143–157, 2001.

[27] Y. Yuan, B. M. Chesnutt, W. O. Haggard, and J. D. Bumgardner, "Deacetylation of chitosan: material characterization and in vitro evaluation via albumin adsorption and pre-osteoblastic cell cultures," *Materials*, vol. 4, no. 8, pp. 1399–1416, 2011.

[28] G. Qun and W. Ajun, "Effects of molecular weight, degree of acetylation and ionic strength on surface tension of chitosan in dilute solution," *Carbohydrate Polymers*, vol. 64, no. 1, pp. 29–36, 2006.

[29] N. T. Le, J. M. Myrick, T. Seigle, P. T. Huynh, and S. Krishnan, "Mapping electrospray modes and droplet size distributions for chitosan solutions in unentangled and entangled concentration regimes," *Advanced Powder Technology*, vol. 29, no. 12, pp. 3007–3021, 2018.

[30] Y. Jiang, C. Fu, S. Wu, G. Liu, J. Guo, and Z. Su, "Determination of the deacetylation degree of chitooligosaccharides," *Marine Drugs*, vol. 15, no. 11, Article ID 332, 15 pages, 2017.

[31] R. Czechowska-Biskup, D. Jarosińska, B. Rokita, P. Ulański, and J. M. Rosiak, "Determination of degree of deacetylation of chitosan - comparision of methods," *Progress on Chemistry and Application of Chitin and its Derivatives*, vol. 2012, pp. 5–20, 2012.

[32] I. A. Sogias, V. V. Khutoryanskiy, and A. C. Williams, "Exploring the factors affecting the solubility of chitosan in water," *Macromolecular Chemistry and Physics*, vol. 211, no. 4, pp. 426–433, 2010.

[33] Y. Jampafuang, A. Tongta, and Y. Waiprib, "β-Impact of crystalline structural differences between α- and β-chitosan on

their nanoparticle formation via ionic gelation and superoxide radical scavenging activities," *Polymers*, vol. 11, no. 12, 2019.

[34] R. Czechowska-Biskup, R. A. Wach, J. M. Rosiak, and P. Ulański, "Procedure for determination of the molecular weight of chitosan by viscometry," *Progress on Chemistry and Application of Chitin and its Derivatives*, vol. 23, 2018.

[35] S. Fuentes, P. J. Retuert, A. Ubilla, J. Fernandez, and G. Gonzalez, "Relationship between composition and structure in chitosan-based hybrid films," *Biomacromolecules*, vol. 1, no. 2, pp. 239–243, 2000.

[36] J. Kumirska, M. Czerwicka, Z. Kaczynski et al., "Application of spectroscopic methods for structural analysis of chitin and chitosan," *Marine Drugs*, vol. 8, no. 5, pp. 1567–1636, 2010.

[37] X. Li, M. Yang, X. Shi et al., "Effect of the intramolecular hydrogen bond on the spectral and optical properties in chitosan oligosaccharide," *Physica E: Low-Dimensional Systems and Nanostructures*, vol. 69, pp. 237–242, 2015.

[38] C. Dwivedi, I. Pandey, H. Pandey et al., "Electrospun nanofibrous scaffold as a potential carrier of antimicrobial therapeutics for diabetic wound healing and tissue regeneration," *Nano- and Microscale Drug Delivery Systems*, 2017.

[39] O. Budishevska, N. Popadyuk, A. Musyanovch et al., "Formation of three-dimensional polymer structures through radical and ionic reactions of peroxychitosan," *Studies in Natural Products Chemistry*, vol. 64, 2020.